ELECTROMAGNETIC RESPONSE FUNCTIONS OF FEW–NUCLEON SYSTEMS

V.D. EFROS[1) 2)], W. LEIDEMANN[1) 3)], G. ORLANDINI[1) 3)]
AND E.L. TOMUSIAK[4)]

[1)] *Dipartimento di Fisica, Universitá di Trento*
I–38050 Povo, Italy
[2)] *Russian Research Centre "Kurchatov Institute"*
1213182 Moscow, Russia
[3)] *Istituto Nazionale di Fisica Nucleare, Gruppo collegato di Trento, Italy*
[4)] *Department of Physics and Engineering Physics*
and Saskatchewan Accelerator Laboratory,
University of Saskatchewan, Saskatoon, Canada S7N 0W0

Inclusive electromagnetic reactions in few–nucleon systems are studied basing on accurate three– and four–body calculations. The longitudinal ^{4}He(e,e') response function obtained at $q \leq 600$ MeV/c completely agrees with experiment. The exact ^{4}He spectral function obtained in a semirealistic potential model is presented, and the accuracy of the quasielastic response calculated with its help is assessed, as well as the accuracy of some simpler approximations for the response. The photodisintegration cross section of ^{3}He obtained with the realistic AV14 NN force plus UrbanaVIII NNN force agrees with experiment. It is shown that this cross section is very sensitive to underlying nuclear dynamics in the $E_\gamma \simeq 100$ MeV region. In particular, the NNN nuclear force clearly manifests itself in this region.

1 Introduction

Our recent results on the ^{4}He(e,e') process and the photodisintegration cross sections of trinucleons are presented in the talk. The issues of interest are the accuracy of the conventional 4N formulation for the ^{4}He(e,e') reaction and the accuracy of its description in the framework of the spectral function approximation, the sensitivity of the photodisintegration cross section to the choice of NN interaction, and the manifestation of NNN force in the process. The quantities we study are response functions having e.g. in the (e,e') case the form

$$R(q,\omega) = \bar{\sum}_{M_0} \int df |\langle \Psi_f | \hat{O}(\mathbf{q}) | \Psi_0(M_0) \rangle|^2 \delta[\omega - (E_f + q^2/(2Am) - E_0)], \quad (1)$$

q and ω being momentum and energy transferred to the nucleus. We avoid calculating the complete set of final states Ψ_f, and we obtain the response functions with the method explained in refs. [1,2] requiring only bound–state type calculations. Within the adopted formulation of the problem the numeri-

cal results below are accurate at the per cent level.

2 The (e, e') response and spectral function of ^{4}He

In the present report, we present the results on the ^{4}He(e, e') response in the q range of 300–600 MeV/c. Additional information can be found in [2,3,4,5]. A non–relativistic 4N Hamiltonian with central NN potentials reproducing the $^1S_0$ and $^3S_1$ NN phase shifts up to high energy has been used as a dynamic input. This Trento (TN) potential is listed in Ref. [2]. The conventional single–particle transition operator that includes the Sachs form factors $G_E^{p,n}$ with the usual relativistic correction has been adopted. No further approximations have been used, and the FSI is thus fully taken into account. In Fig. 1 the calculated longitudinal response function $R_L(q, \omega)$ is shown with solid curves for four values of the transferred momentum q [MeV/c] along with the Bates [6] and Saclay [7] data. (The results for $q \leq 500$ MeV/c differ a bit from those in Refs. [3,4] due to minor corrections in the formulation, see [5].) One observes a very good agreement with experiment in the whole range of q values. (A drop in the data at $q = 500$ MeV/c in the vicinity of ω =250 MeV is at variance with the sum rule systematics.)

To interpret the results obtained let us estimate the maximal momenta in the initial state contributing substantially to the response. Let us consider e.g. the final state component in which only the N–$(A-1)$ relative motion is fast. It is sufficient here to consider this relative motion in the plane wave approximation. Let $\mathbf{k}_{rel}$ be the relative momentum between the fast nucleon and the remaining $(A-1)$ subsystem. The FSI admixes the momenta lying in the range $\mathbf{k}_{rel} + \Delta\mathbf{k}$ to $\mathbf{k}_{rel}$. The momenta $\Delta\mathbf{k}$ are determined by the nuclear force, and they are lower than $\mathbf{k}_{rel}$ values of interest for us. We have $\mathbf{k}_{rel} = [(A-1)/A][\mathbf{k}_N - (A-1)^{-1}\mathbf{K}_{A-1}] = \mathbf{k}_N - A^{-1}\mathbf{K}_A$. The corresponding single–particle momentum probed in the ground state is $\mathbf{k}_{miss} \equiv \mathbf{k}_{rel} - \mathbf{q}(A-1)/A$. The predominant contribution comes from the states with $\mathbf{k}_{rel}$ directed along $\mathbf{q}$. Using the energy conservation in the form $\omega \simeq k_{rel}^2 A/[2(A-1)m] + q^2/(2Am) - E_{gs}$ and setting $\omega + E_{gs} = q^2/(2m) + \Delta$ one obtains $k_{miss} \simeq [(A-1)/A]|\{q^2 + [A/(A-1)]2m\Delta\}^{1/2} - q|$. Let us consider the right wing of the response. Setting, for example, $q = 600$ MeV/c, Δ =100 MeV, c.f. Fig. 1, one gets $k_{miss} = 0.7$ fm^{-1}. As a consequence, only low momenta in the nuclear interaction play a role in the kinematical region considered. Contributions from other reaction mechanisms cannot change this conclusion. The semirealistic NN potentials of the type we used probably lead to the same low momentum content of the wave functions as the fully realistic NN interactions. This is illustrated in Fig. 2 where the single–particle momen-

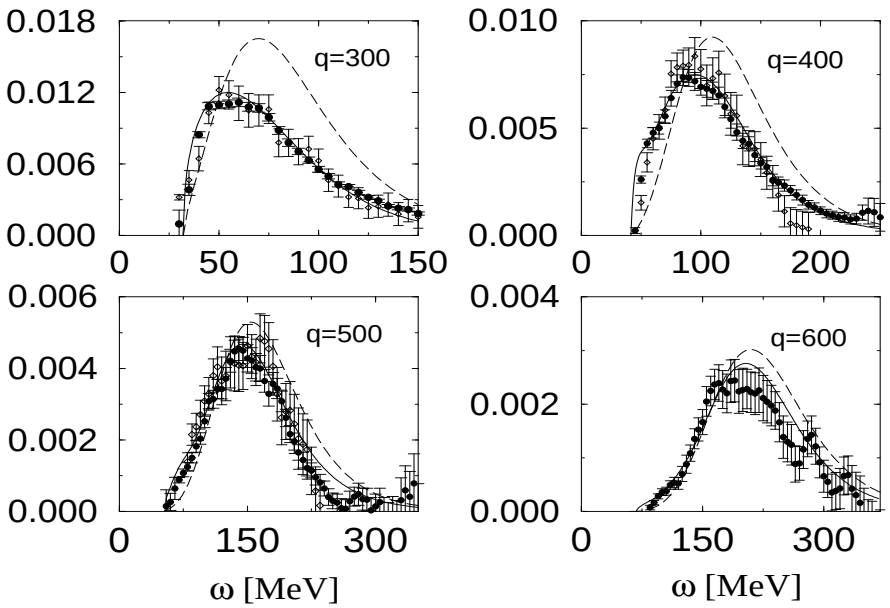

Figure 1. Longitudinal response of ^{4}He in MeV^{-1}. Full results: solid curves, PWIA calculation: dashed curves. Bates and Saclay data are represented with open diamonds and closed circles, respectively.

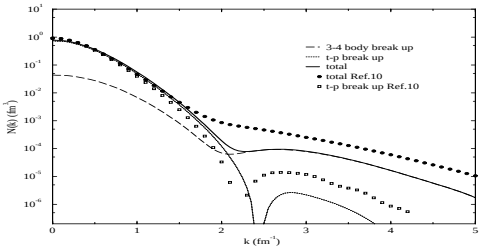

Figure 2. Total and partial momentum distributions of ^{4}He with the TN potential and with Argonne v_{18}+Urbana IX [10].

tum distribution of ^{4}He for our NN potential is compared with that obtained from a realistic nuclear force [10]. The agreement above with experiment at the right wing of the response then testifies to a correct description of the corresponding low–momentum content of the wave functions within the adopted 4N formulation. It shows the applicability of the conventional form of the electro-

magnetic interaction as well. On the contrary, rather high nucleon momenta in the ground–state wave function are probed at the left wing of the response at high q and small ω [8].

The SF of ^{4}He and the corresponding QE response have also been calculated exactly with the same NN potential. The SF $S(k,E)$ represents the joint probability of finding a nucleon with momentum $\mathbf{k}$ and a residual $(A-1)$ system with energy $E+E_{gs}$:

$$S_{t_z}(k,E) = \bar{\sum_{M_0,s_z}} \int df |\langle \Psi_f^{A-1}; \mathbf{k} s_z t_z | \Psi_0^A(M_0)\rangle|^2 \delta[E-(E_f^{A-1}-E_0^A)]. \quad (2)$$

Here s_z and t_z are the spin and isospin quantum numbers of the nucleon, E_f^{A-1} and Ψ_f^{A-1} are eigenvalues and eigenstates of the $(A-1)$ system, and E_0^A and Ψ_0^A are such quantities for the ground state. The energy E can be viewed as the removal energy of the nucleon. The calculation of the SF from its definition requires obtaining the complete set of states of the residual $(A-1)$ subsystem. Previously the spectral function has been calculated in the A=3 case, which is essentially the two–body problem, and, approximately, for nuclear matter, see [9] for the references. We have avoided calculating the complete set of $A=3$ continuum states with the help of the approach mentioned in Sec. 1. The proton SF $S_p(k,E)$ thus obtained is shown in Fig. 3. It includes two

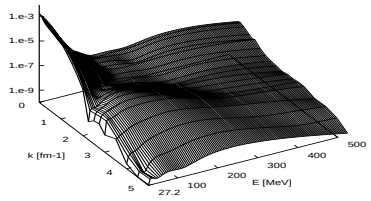

Figure 3. SF $S_p(k,E)$ of ^{4}He with TN potential in units of fm^3 MeV^{-1}.

contributions: from the $A=3$ rest subsystem in the ground state, and in the continuum, c.f. Eq. (4) below. The first of these is determined by the corresponding momentum distribution, and the second one is shown in the figure. The values of $S_p(k,E) \geq E_{thr}^{A-1}+1$ MeV are plotted. (We note that $S_p(k,E_{thr}^{A-1})=0$ and thus $S_p(k,E)$ exhibits a strong slope at low energy.) For momenta below 2 fm^{-1} one finds a sharp maximum at about 2 MeV above E_{thr}^{A-1}. In Fig. 4 the cut of the calculated spectral function at $k=0.25$ fm^{-1} is shown. These results appear to have subsequently been confirmed experimentally [11]. For $k>2$ fm^{-1} the calculated spectral function exhibits a

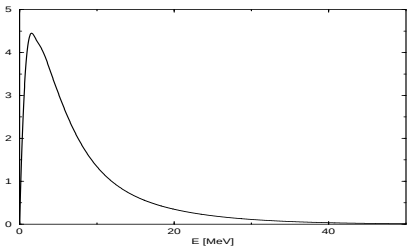

Figure 4. The cut of the ^{4}He SF at $k = 0.25$ fm^{-1}. The values of SF are in $10^{-3}\cdot$ fm^3 MeV^{-1}.

ridge where the peak position shifts to higher E for increasing k. This ridge should presumably correspond to a proton struck from the region of a strong two–nucleon correlation, see [9,12].

The QE response

$$R_L^{qe}(q,\omega) = A[\tilde{G}_E^p(Q)]^2 \int d\mathbf{k} dE S_p(k,E)$$
$$\times\delta[\omega - E - (\mathbf{k}+\mathbf{q})^2/(2m) - k^2/[2(A-1)m]]. \quad (3)$$

is shown in Fig. 1 with the dashed curve. At $q = 600$ MeV/c the height of the peak is overestimated by about 9% in the framework of the QE approximation. At low ω, the PWIA assumption inherent to R_L^{qe} obviously breaks down. For high ω, the relative role of disregarded lower momenta admixtures in the final state wave function increases with ω. Due to these reasons the relative error of the QE approximation (3) increases at the wings of the response. It is seen from Fig. 1 that the QE peak is shifted to higher energies with respect to the true one. The shift of the peak can be qualitatively understood considering a nucleon at rest in a potential well: ω can be estimated as $q^2/(2m) + V_f(q) - V_i$, where $V_{f,i}$ are the potential energies before or after interaction with the virtual photon. While V_f is negative, it becomes zero in PWIA leading to an increase in ω.

It is advantageous to have a simple and good approximation for the QE response. One can write

$$S(k,E) = n_{tp}(k)\delta[E - E_0(^3\mathrm{H}) + E_0(^4\mathrm{He})] + S_{inel}(k,E). \quad (4)$$

Here the first term represents the residual $A = 3$ system in the ground state, and we do not differentiate between the t-p and n-^{3}He channels. The second term is depicted in Fig. 3 and represents the contribution of the residual $A = 3$ system being in continuum. It is seen from Fig. 3 that for low k relevant

to us almost all the strength in S_{inel} is concentrated close to the thershold $E = E_{min}$. This suggests the approximation (to be put into Eq. (3))

$$S(k,E) \simeq n_{tp}(k)\delta[E - E_0(^3\mathrm{H}) + E_0(^4\mathrm{He})] + n_{t^*p}(k)\delta[E - E_{t^*p} + E_0(^4\mathrm{He})] \quad (5)$$

where E_{t^*p} is the threshold breakup energy of the residual nucleus. Using (5) one does not need continuum state calculations since $n_{t^*p}(k) = n(k) - n_{tp}(k)$. One obtains an even simpler approximation considering that $E_{t^*p} \simeq E_0(^3\mathrm{H})$:

$$S(k,E) \simeq n(k)\delta[E - E_0(^3\mathrm{H}) + E_0(^4\mathrm{He})]. \quad (6)$$

Eq. (6) was used in the literature (see e.g. [13]). One may note that at the small k values of interest the term S_{inel} in (4) is only of secondary importance (e.g. the integrated values of n_{tp} and n_{t^*p} equal 0.89 and 0.11, respectively,) which improves the quality of the approximations (5), (6). In Fig. 5 we show the

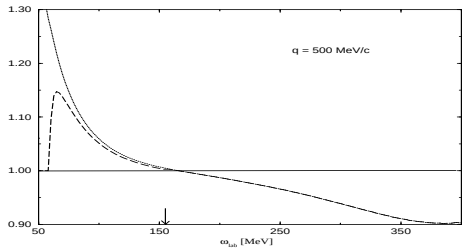

Figure 5. QE response (3) with the SF of Eq. (5) (dashed curve) and of Eq. (6) (dotted curve) relative to that with the full SF (the QE peak is marked by an arrow).

responses (3) obtained with these approximations relative to Eq. (3) with the full spectral function. Except for small ω where the wrong threshold behavior in Eq. (6) may play a role, the three responses are very similar, particularly in the peak region. (At q = 300, 400, and 1000 MeV/c one has very similar results.)

3 Total photodisintegration cross sections of trinucleons

Earlier theoretical work on the photodisintegration cross section of trinucleons in a wide energy range is outlined in Ref. [14]. The first rigorous calculations have been performed with separable central potentials. Mixed symmetry states have been disregarded even though they play an important role in the process. Approximate calculations of the three–body breakup with low–energy central local potentials were also performed. In [15] the cross section has been obtained with a non–central potential but only the three lowest hyperspherical terms in

the expansion of continuum wave functions were retained which may influence the results. In [16] the ^{3}H two–body photodisintegration differential cross sections at $\theta = 90^o$ were calculated with Paris and Bonn NN realistic potentials for $E_\gamma \leq 40$ MeV. In [14] accurate calculations of the total cross sections have been performed with central TN and Malfliet–Tjon (MT) [17] potentials reproducing the s–wave phase shifts up to high energy.

In the present work we calculate the total photodisintegration cross section with realistic NN interactions for the first time and we include an NNN force in addition. As in [14], the approach outlined in Sec. 1 has been used. The calculations are performed for photon energies up to pion threshold, and we pay special attention to the high energy tail of the cross section. We obtain a sizeable contribution of NNN force to the cross section and also comment on the sensitivity to the NN force. It may be natural to expect some sensitivity to the NN force since if one takes, for example, E_γ =110 MeV and considers the N+d breakup then the N−d relative momentum is about 1.9 fm^{-1}, and single–particle momenta in $\hat{O}\Psi_0$ of this size may be probed in the process.

The calculation was done with a non–relativistic three–nucleon Hamiltonian. The realistic NN interactions AV14 [18] and TRSB [19] were employed. These NN interactions underbind ^{3}H by about 0.8 MeV and 1 MeV, respectively. In the third version of the calculation, the AV14 NN interaction plus NNN UrbanaVIII force are used. Along with these results the cross sections [14] with central TN and MT potentials are listed as well.

For the latter potentials, as well as in the case of the softer core TRSB interaction, we used the Jastrow correlated hyperspherical basis [20]. The correlations speed up the convergence but not to a sufficient degree in case of the stronger core AV14 interaction. In the Jastrow case, one chooses the two–body correlation function as the mean value of the triplet and singlet NN low–energy wave functions. However, for interactions like AV14 it is advantageous to take into account differences between correlations in different two–nucleon spin–isospin states. One possibility is to use different Jastrow factors at different groups of basis states before symmetrization [21]. However, after symmetrization the correlations then lose their role as correlations in given NN states and become some effective correlations which still may substantially speed up the convergence [21] due to the many variational parameters involved. Such a procedure is not convenient in our case since our response calculations are not variational ones. In the present work, in the AV14 case, we use a new version of a correlated basis. Spin–isospin dependent correlations are used, and they retain their role as correlations in the given four spin–isospin NN states, see [22]. In Table 1 the properties of our ground state wave function of ^{3}H are listed in comparison with Ref. [23]. The UrbanaVIII potential was taken as the NNN

Table 1. Bound–state properties of ^{3}H with the AV14 interaction

	E_b, MeV	r_{rms}, fm	$P(D)$, %	E_b(NN+NNN), MeV
present work	7.71	1.66	8.85	8.52
Ref. [23]	7.67	1.67	8.96	8.46

force in the last column.

In the present work we confine ourselves with the unretarded E1 approximation for the transition operator which is known to be a very good one for the total cross section at least for not too high energies. Within this approximation the transition current operator may be rewritten exactly as the dipole moment operator of a system, while MEC currents are taken into account automatically. In Fig. 6 our total photodisintegration cross section of ^{3}He calculated

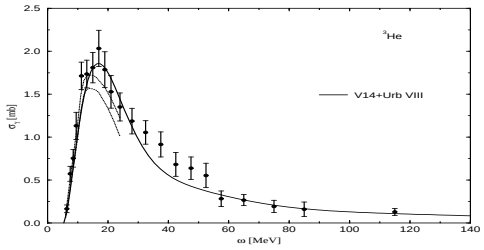

Figure 6. Photodisintegration cross section of ^{3}He. Theoretical curve is obtained with the AV14+UrbanaVIII nuclear force (full curve). Experimental data are of Refs. [24] (filled circles) and [25] (upper and lower bound delineated with dotted curves).

with AV14+UrbanaVIII interaction is shown along with experimental data. The theory leads to an agreement with the data of Ref. [24]. In Fig. 7 our results in the tail region of the ^{3}H cross section are shown. Separate cross sections for transitions to final states with isospin $T = 1/2$ and $3/2$ are presented. Transitions to $T = 3/2$ correspond to the three–body breakup while those to $T = 1/2$ are known to correspond predominantly to the two–body breakup. One sees a large difference between predictions of different models in this region. In the $T = 1/2$ case, realistic NN interactions lead to much higher cross section than central NN forces. This can be attributed to tensor correlations produced by realistic interactions. It is also seen that the NNN nuclear force clearly manifests itself by leading to a sizable further increase in the cross section. As to the $T = 3/2$ case, the interesting point is that the cross section obtained with the realistic TRSB NN interaction is close to those for the central NN potential models but strongly differs from that obtained with

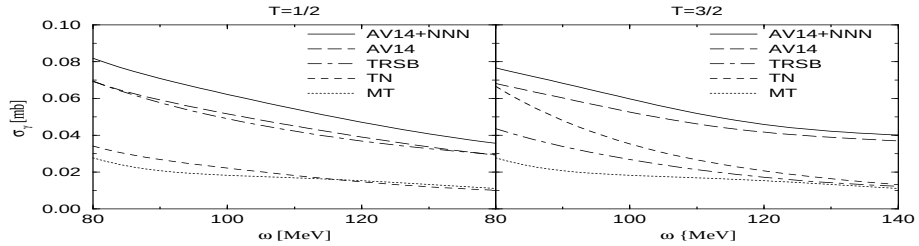

Figure 7. Photodisintegration of ^{3}H. Results with various choices of nuclear interactions. The UrbanaVIII potential was taken as the NNN force.

AV14. We are planning to consider other realistic NN interactions as well to clear out a sensitivity to the choice of NN interaction.

There exist only two experimental data points in the energy range presented in Fig. 7 (see Fig. 6, the ^{3}He and ^{3}H cross sections are practically indistinguishable in this region [14]). These experimental data are in favour of the AV14+UrbanaVIII interaction. Our results thus show that, in contrast to many quantities conventionally studied in few–nucleon physics, an experimental study of the process in the considered energy region may allow a clear discrimination between various models of NN interaction and detection of the contribution of NNN force. Corrections from retardation and the contribution of other multipoles will be studied separately. They are rather small, and they cannot change the conclusion about high sensitivity of the process to nuclear dynamics. Obviously, one can anticipate even more sensitivity to nuclear dynamics in exclusive experiment.

References

1. V.D. Efros, W. Leidemann and G. Orlandini, *Phys. Lett. B* **338**, 130 (1994); *Nucl. Phys. A* **631**, 658c (1998); V.D. Efros, *Phys. At. Nucl* (in press).
2. V.D. Efros, W. Leidemann and G. Orlandini, *Few–Body Sys.* **26**, 251 (1999).
3. V.D. Efros, W. Leidemann and G. Orlandini, *Phys. Rev. Lett.* **78**, 432 (1997).
4. V.D. Efros, W. Leidemann and G. Orlandini, Proc. of the Conf. on *Perspectives in Hadronic Physics*, ICTP, Trieste, 12–16 May 1997. World Scientific, p. 94.
5. V.D. Efros, W. Leidemann and G. Orlandini, *Phys. Rev. C* **58**, 582 (1998).

6. S.A. Dytman et al., *Phys. Rev. C* **34**, 800 (1988).
7. A. Zghiche et al., *Nucl. Phys. A* **572**, 513 (1994).
8. W. Czyz and K. Gottfried, *Ann. Phys.* (N.Y.) **45**, 47 (1963).
9. C. Ciofi degli Atti and S. Simula, *Phys. Rev. C* **53**, 1689 (1996).
10. A. Arriaga, V.R. Phandharipande and R.B. Wiringa, *Phys. Rev. C* **52**, 2362 (1995).
11. S. Gilad et al., Proc. of the Conf. on Nuclear and Particle Physics with CEBAF at Jefferson Lab., Dubrovnik, Nov. 1998, Fizika (in press).
12. L.L. Frankfurt and M.I. Strikman, *Phys. Rep.* **76**, 215 (1981); **160**, 235 (1988).
13. J. Carlson and R. Schiavilla, *Phys. Rev. Lett.* **68**, 3682 (1992).
14. V.D. Efros, W. Leidemann and G. Orlandini, *Phys. Lett. B* **408**, 1 (1997).
15. A.N. Vostrikov and M.V. Zhukov, *Sov. J. Nucl. Phys.* **34**, 196 (1981).
16. W. Schadow and W. Sandhas, *Phys. Rev. C* **55**, 1074 (1997).
17. R.A. Malfliet and J. Tjon, *Nucl. Phys. A* **127**, 161 (1969).
18. R.B. Wiringa, R.A. Smith and T.L. Ainsworth, *Phys. Rev. C* **29**, 1207 (1984).
19. R. de Tourreil, B. Rouben and D.W.L. Sprung, *Nucl. Phys. A* **242**, 445 (1975); J. Côte, R. De Tourreil, B. Rouben and D.W.L. Sprung, *Nucl. Phys. A* **273**, 269 (1976).
20. Yu.I. Fenin and V.D. Èfros, *Sov. J. Nucl. Phys.* **15**, 497 (1972).
21. A. Kievsky, M. Viviani and S. Rosati, Nucl. Phys. **A551**, 241 (1993).
22. W. Leidemann ei al., Proc. of the Conf. on Nuclear and Particle Physics with CEBAF at Jefferson Lab., Dubrovnik, Nov. 1998, Fizika (in press).
23. C.R. Chen, G.L. Payne, J.L. Friar and B.F. Gibson, *Phys. Rev. C* **31**, 2266 (1985); R.B. Wiringa, *Phys. Rev. C* **43**, 1585 (1991).
24. V.N. Fetisov, A.N. Gorbunov and A.T. Varfolomeev, *Nucl. Phys. A* **71**, 305 (1965).
25. D.D. Faul, B.L. Berman, P.Meyer and D. Olson, *Phys. Rev. C* **24**, 849 (1981).